Supporting Information

Woodward et al. 10.1073/pnas.1214530110

SI Materials and Methods

***Xenopus laevis* Oocytes.** Oocytes were removed from female pigmented *X. laevis* (Xenopus-1 Inc.) and defolliculated using collagenase A (Roche) in a Ca^{2+}-free OR-2 ringer solution. Stage V–VI oocytes were selected and injected (Nanoinject II, Drummond Scientific) with 50 nL mRNA. Oocytes after injection were cultured in a modified L-15 media (OR-3) and kept at 15–20 °C. mRNA was prepared using the SP6 mMessage mMachine (Ambion Inc.) according to the manufacturer's protocol.

Cell Culture Protocol. Human embryonic kidney 293 (HEK293) cells were cultured in DMEM (Invitrogen/Gibco; 11995), and CHO cells were cultured in Ham's F-12 (Cellgro; 10–080-cv); both were supplemented with 10% FBS and penicillin and streptomycin (500 and 50 mg/mL, respectively).

Cell Transfection Protocol. Cells were grown to >90% confluence overnight, and plasmid was transfected using Lipofectamine 2000 (Invitrogen; catalog no. 11668–019) according to the manufacturer's protocol. Medium was changed back to regular cell growth medium 5 h after transfection.

Western Blot Protocol. Cells were lysed 24 h post transfection using lysis buffer [1% (vol/vol) deoxycholic acid, 1% (vol/vol) Triton X-100, 0.1% (vol/vol) SDS, 150 mM NaCl, 1 mM EDTA, 10 mM Tris·HCl (pH 7.5), and protease inhibitor (complete protease inhibitor; Roche)]. The samples were incubated at 37 °C for 30 min with 2× Laemmli buffer, with or without the reductant 5% 2-β mecaptoethanol. The samples were run on precast gels of either 4–15% or 7% (Bio-Rad), transferred to PVDF membrane (Bio-Rad; 162–0177), and blocked in 5% nonfat milk. The appropriate primary antibody [anti-breast cancer resistance protein (BCRP); Millipore Corp., clone BXP-21, 1:200; anti-GAPDH, Sigma, 1:6,000 as loading control] was added, and the membrane was incubated overnight at 4 °C. After washing and the addition of appropriate secondary antibody, the membrane was exposed with super signal (Pierce), the chemiluminesence signal was captured using Fuji Film Intelligent Dark Box LAS-3000 (GE), and band density was calculated using National Institutes of Health Image. For the quantitative Western blots, we used the fluorescent secondary anti-mouse antibody Alexa fluor 488 at 1:5,000 (Invitrogen) and the Bio-Rad Pharos FX imaging system with Bio-Rad Quality One imaging software.

Western Blot Protocol for *Xenopus* Oocytes. Four days after injection, 10 oocytes per treatment were pooled and placed into a 1.5-mL tube. Ice-cold oocyte lysis buffer was added (in mM: 20 Tris·HCl, 140 NaCl, 2% Triton X-100, and protease inhibitors), and the oocytes were incubated on ice for 30 min. Then the oocytes were homogenized and spun at 4 °C at 7,500 × *g* to remove the nucleus and membrane portions. The cell lysate was then stored at −80 °C until used for the Western blot. A BCRP antibody was used to probe the blot (anti-BCRP; Millipore, clone BXP-21 at 1:200), and an anti-actin antibody (1:1,000) was used as a loading control.

Surface Biotinylation Protocol. Twenty-four hours post transfection, cells are washed four times with ice-cold PBS containing 0.1 mM $CaCl_2$ and 1 mM of $MgCl_2$. The cells were then incubated with 1 mg/mL Sulpho-NHS-SS-biotin (Pierce catalog no. 21331) for 1 h at 4 °C. The biotin was quenched with three washes of 192 mM glycine (GibcoBRL; 15527–013) in PBS at 4 °C. The cells were lysed using lysis buffer, and an aliquot of lysate was taken for total protein measurement. To the remaining sample, ultra-link immobilized NeutrAvidin beads (Pierce; catalog no. 53150) were added, and samples were incubated at 4 °C for 2 h and washed with lysis buffer, and the bound surface proteins were eluted from the beads with 50 μL of 2× loading buffer incubating at 42 °C for 30 min.

ABCG2 Nucleotide-Binding Domain Homology Model. Multiple-sequence alignment was done using COBALT (1) and shown in Fig. S3. The homology model of the ATP-binding cassette subfamily G 2 (ABCG2) nucleotide-binding domain (NBD) (residues 45–275) was built using the Swiss-Model server (2) and sequences of Sav1866 (3), human cystic fibrosis transmembrane conductance regulator (CFTR) minimal NBD1 (4), mouse CFTR NBD1 (5), and ABC transporter hemolysin B (HlyB) (6) as templates. The resulting models were similar, and in each case the conserved Walker A, Walker B, LSGGQ, and Q-loop motifs were aligned. The model based on Sav1866 was selected for further work because it was in a whole-protein context, had the best Z-score (7), and better positioned the ABCG2 His-243 (in the H-loop) with respect to bound nucleotide. The initial model had seven residues with unfavorable φ- and ψ-angles (8) in loop regions and was further refined using the GalaxyWEB server (9). The refined model has a Z-score of −2.179, no residues with unfavorable φ- and ψ-angles, and rmsd values with Sav1866, human CFTR minimal NBD1, and mouse CFTR NBD1 of 0.6, 1.8, and 2.0 Å, respectively.

Immunocytochemistry Protocol. Cells were grown on glass coverslips and transiently transfected with plasmid using Lipofectamine 2000. Then they were washed with ice-cold PBS with 0.1 mM $CaCl_2$ and 1.0 mM $MgCl_2$ (PBS C/M) three times and fixed with 4% paraformaldehyde (Electron Microscopy Sciences; 15710 16% solution) for 15 min at room temperature. Coverslips were then washed with ice-cold PBS C/M three times and permeabilized with 0.25% Triton X-100 (SigmaUltra T9284) for 10 min at room temperature. Coverslips were then washed with ice-cold PBS C/M three times and blocked with 5% goat serum for 40 min. Cells were then incubated with primary antibody against ABCG2 (anti-BCRP monoclonal antibody; Millipore clone BXP-21, 1:100) in 5% goat serum for 40 min. Cells were then washed with PBS C/M for 5 min three times and incubated with secondary antibody (Cy3 secondary antibody; Sigma, 1:200) in 5% goat serum for 30 min. Cells were then washed with 2.7% NaCl in PBS for 2 min followed by three 5-min washes with ice-cold PBS C/M. The coverslips were mounted onto glass slides after adding mounting antifade medium (Vectashield with DAPI H-1200; Vector Labs). Images were taken with 63× magnification using a Zeiss 510 Meta no. 2 confocal microscope (The Microscope Facility of The Johns Hopkins University School Of Medicine).

Deglycosylation Protocol. For PNGase F, twenty-four hours post transfection, cells were lysed, and total protein was harvested and estimated. Ten micrograms of total protein was denatured in 10× buffer by heating at 100 °C for 10 min. The denatured mix was then treated with 10XG7, 10% Nonidet P-40, PNGase F (New England Biolabs; P0704S), and H_20 and incubated at 37 °C for 1 h. At the end of the reaction, the sample was analyzed by Western blot. For endoglycosidase H (EndoH), 10 μL of total protein sample was denatured as above. The denatured mix was then treated with 10XG5, EndoH (New England Biolabs; P0702S), and H20 and incubated at 37 °C for 1 h. At end of the reaction, the sample was analyzed by Western blot.

Statistical Analysis. Statistical comparisons of density measurements from Western blots were done with the Student's *t* test for

pair-wise comparisons or with an ANOVA used with a Tukey's test for all multiple comparisons. All reported means are ± SEM.

Constructs and Subcloning. All constructs were generated from a wild-type ABCG2 containing the pcDNA3.1 plasmid created from a BCRP *Xenopus* expression plasmid (10). All point mutations and deletions were performed using the Stratagene QuikChange Site-Directed Mutagenesis kit. All primers were ordered from Invitrogen (Life Technologies). The plasmid with appropriate sequence was transformed into competent cells for plasmid amplification. The following primers were used: (*i*) Q141K primers (FW—5′-ggtgagagaaaacttaaagttctcagcagctc-3′; RV—5′-gagctgctgagaactttaagttttctctcacc-3′); (*ii*) G188E primers (FW—5′-ccgtggtgtgtctgaaggagaaagaaaaag-3′; RV—5′- ctttttctttctccttcagacacaccacgg-3′); (*iii*) R193K primers (FW—5′-gtctggaggagaaagaaaaaagactagtataggaatggag-3′; RV—5′- ctccattcctctactagtctttttttctttctcctccagac-3′); (*iv*) ΔF142 primers (FW—5′-gagaaaacttacagtcagcagctcttcggc-3′; RV—5′-gccgaagagctgctgactgtaagttttctc-3′); (*v*) K473E primers (FW—5′-gtgtcatcttatttccttggag aactgttatctgatttattacc-3′; RV—5′-ggtaataaatcagataacagttctccaaggaaataagatgacac-3′); (*vi*) K473P primers (FW—5′- gtgtcatcttatttccttggac cactgttatctgatttattaccc-3′; RV—5′-gggtaataaatcagataacagtggtccaaggaaataagatgacac-3′); (*vii*) K473W primers (FW—5′-gtgtcatcttatttccttggatggctgttatctgatttattacc-3′; RV—5′-gggtaataaatcagataacaggcatccaaggaaataagatgaca-3′).

C-14 Uric Acid Transport Assays. ***Accumulation studies.*** Cells were grown to 100% confluence and transfected in six-well plates before the experiment began, and photos were taken of each well to normalize accumulation rates to the area covered. Twenty-four hours after transfection, 24-h cells were treated with 10 μM VRT-325 or vehicle for 24 h. The assay began with cells incubated in DMEM containing 500 μM cold urate and 75 μM "hot" C-14–labeled urate (made from 2 mM stock; American Radio-labeled Chemicals); the incubation lasted 120 min at 37 °C, 5% CO_2. The cells were then washed four times with ice-cold DMEM and lysed with 500 μL of 1 M NaOH. The lysate was collected and placed in a scintillation tube along with 5 mL scintillation fluid and counted (LS600 LL; Beckman Coulter Inc.).

Efflux studies. Cells were grown, transfected, and incubated with C-14 uric acid as above. After washing, cells were left at room temperature and allowed to efflux uric acid. Every 5 min for 1 h, the cell media was collected and replaced and the radioactivity counted. At the end of 1 h, the cells were lysed as above and the remaining intracellular C-14 uric acid was measured; the sum of all effluxed counts and remaining counts giving the intracellular C-14 amount at the beginning of the experiment were determined. Because the wild type always began the efflux portion of the experiment with significantly less intracellular urate, we picked time points along the efflux curve where WT and Q141K had equal amounts of intracellular C-14 uric acid and did our comparison on the next 5- min efflux period.

Other Reagents. VRT-325 and Corr-4a were a generous gift from Cystic Fibrosis Foundation Therapeutics and 4-phenylbutyrate was a generous gift from Neeraja Sharma (The Johns Hopkins University School Of Medicine, Baltimore, MD).

1. Papadopoulos JS, Agarwala R (2007) COBALT: Constraint-based alignment tool for multiple protein sequences. *Bioinformatics* 23(9):1073–1079.
2. Arnold K, Bordoli L, Kopp J, Schwede T (2006) The SWISS-MODEL workspace: A web-based environment for protein structure homology modelling. *Bioinformatics* 22(2): 195–201.
3. Dawson RJ, Locher KP (2006) Structure of a bacterial multidrug ABC transporter. *Nature* 443(7108):180–185.
4. Atwell S, et al. (2010) Structures of a minimal human CFTR first nucleotide-binding domain as a monomer, head-to-tail homodimer, and pathogenic mutant. *Protein Eng Des Sel* 23(5):375–384.
5. Lewis HA, et al. (2004) Structure of nucleotide-binding domain 1 of the cystic fibrosis transmembrane conductance regulator. *EMBO J* 23(2):282–293.
6. Zaitseva J, et al. (2006) A structural analysis of asymmetry required for catalytic activity of an ABC-ATPase domain dimer. *EMBO J* 25(14):3432–3443.
7. Benkert P, Biasini M, Schwede T (2011) Toward the estimation of the absolute quality of individual protein structure models. *Bioinformatics* 27(3):343–350.
8. Laskowski RA, MacArthur MW, Moss D, Thornton JM (1993) PROCHECK: A program to check the stereochemical quality of protein structures. *J Appl Cryst* 26:283–291.
9. Ko J, Park H, Heo L, Seok C (2012) GalaxyWEB server for protein structure prediction and refinement. *Nucleic Acids Res* 40(Web Server issue):W294–W297.
10. Woodward OM, et al. (2009) Identification of a urate transporter, ABCG2, with a common functional polymorphism causing gout. *Proc Natl Acad Sci USA* 106(25):10338–10342.

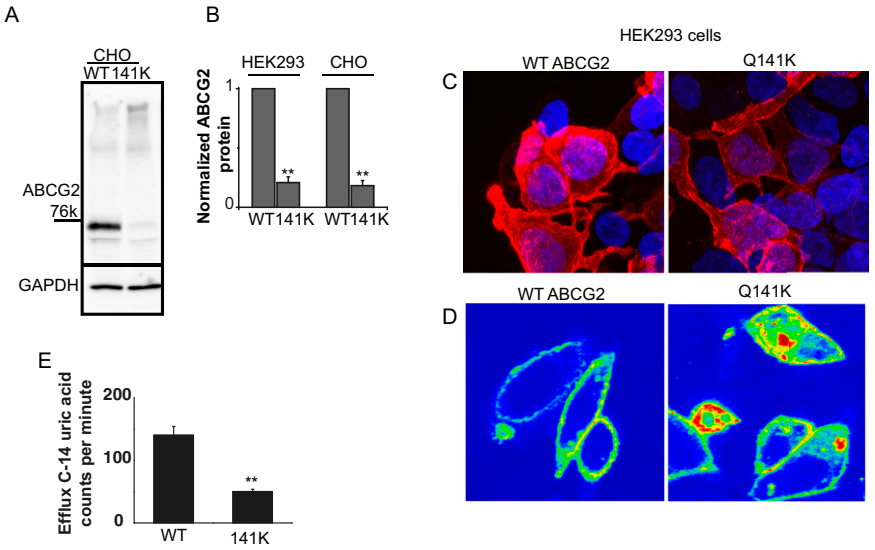

Fig. S1. (*A*) Western blot of transient expression of wild-type (WT) and Q141K ABCG2 protein in CHO cells showing a large decrease in mature mutant Q141K protein. (*B*) Summary data demonstrating in multiple mammalian cell lines that the Q141K mutant total expression is significantly less than WT (CHO: $P < 8.0 \times 10^{-5}$, $n = 4$; HEK293: $P < 0.0007$, $n = 3$). (*C*) Confocal images of WT and Q141K expression in HEK293 cells merged into a single Z-stack image to demonstrate quantity and localization of ABCG2 protein (red signal). DAPI was used to label the nuclei (blue signal). WT ABCG2 expression is greater than Q141K expression and predominantly on or near the surface. (*D*) Single optical confocal sections of HEK293 cells expressing WT or Q141K ABCG2. Heat mapping allows visualization of the majority of protein in the WT at or near the surface whereas, in the Q141K mutant, much of the protein appears to accumulate in the cytosol as aggregates. (*E*) Efflux rates of WT and Q141K ABCG2-expressing HEK293 cells, measured as cpm of C-14 urate efflux. Intracellular urate concentration was the same at the beginning of the 5-min efflux period for both groups ($n = 6$, where $n = 1$ well of a six-well plate covered with ABCG2-expressing HEK293 cells; $P < 9.6 \times 10^{-5}$). All means are ± SEM; $^{**}P < 0.01$.

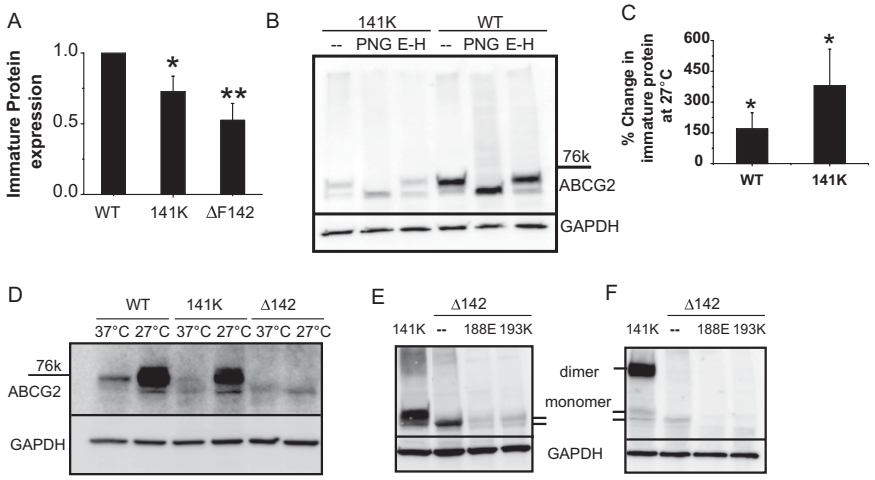

Fig. S2. (*A*) Summary data of expression of immature, unglycosylated ABCG2 wild-type (WT), Q141K, and ΔF142 protein ($n = 5$ for each). (*B*) Representative Western blot of ABCG2 and Q141K ABCG2 subjected to deglycosylation by either PNGase or EndoH; both variants are PNGase-sensitive, but only the mutant Q141K is partially sensitive to EndoH (and thus does not receive complex glycosylation in the Golgi). (*C*) Low-temperature incubation increases immature, unglycosylated WT and Q141K ABCG2 protein (compared with zero, $n = 4$). (*D*) Western blot of protein expression of ABCG2 variants after 48 h of incubation at 27 °C or 37°C ($n = 3$). Suppressor mutations cannot rescue ΔF142 transient expression in HEK293 cells; Western blots of total (*E*) and dimer (*F*) expression of ΔF142 ABCG2 variants ($n = 3$). All means are ± SEM; $^{*}P < 0.05$; $^{**}P < 0.01$.

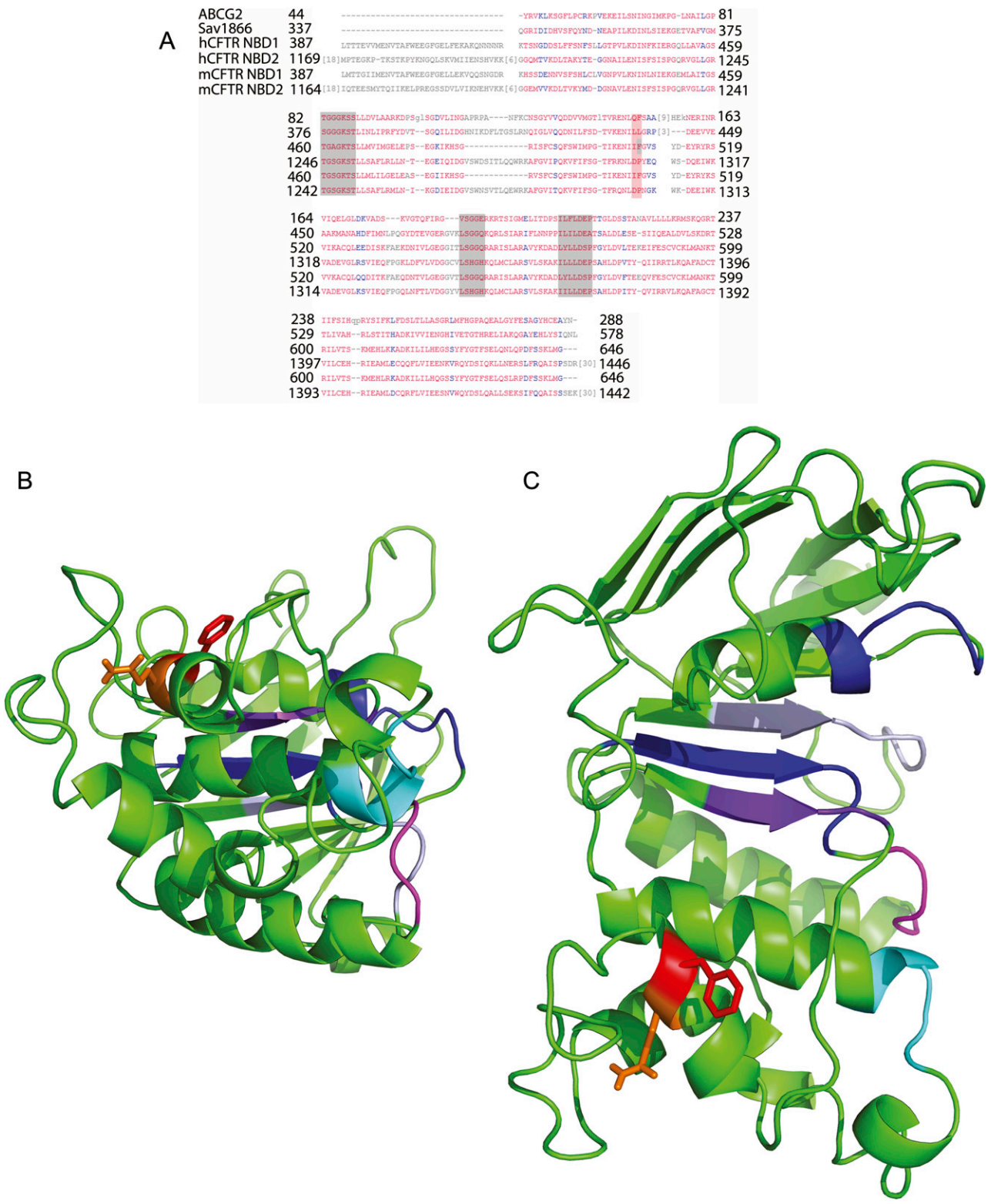

Fig. S3. (*A*) Alignment of nucleotide-binding domains: from top to bottom, ABCG2, Sav1866, human CFTR NBD1, human CFTR NBD2, mouse CFTR NBD1, and mouse CFTR NBD2. Walker A, LSGGQ, and Walker B are highlighted in gray, and Q141 and F142 are in pink. (*B*) ABCG2 NBD homology model with Q141 shown as orange sticks and F142 as red sticks. The NBD dimer interface is approximately on the right and the NBD–TMD interface is approximately on the top. (*C*) Rotation of S2 along the paper plain by 90° and looking down from the NBD–TMD interface. The NBD dimer interface is on the right. For *B* and *C*, the Walker A and B domains are depicted in blue, the H loop in light blue, the Q loop in purple, the D loop in magenta, and the ABC signature region in cyan.

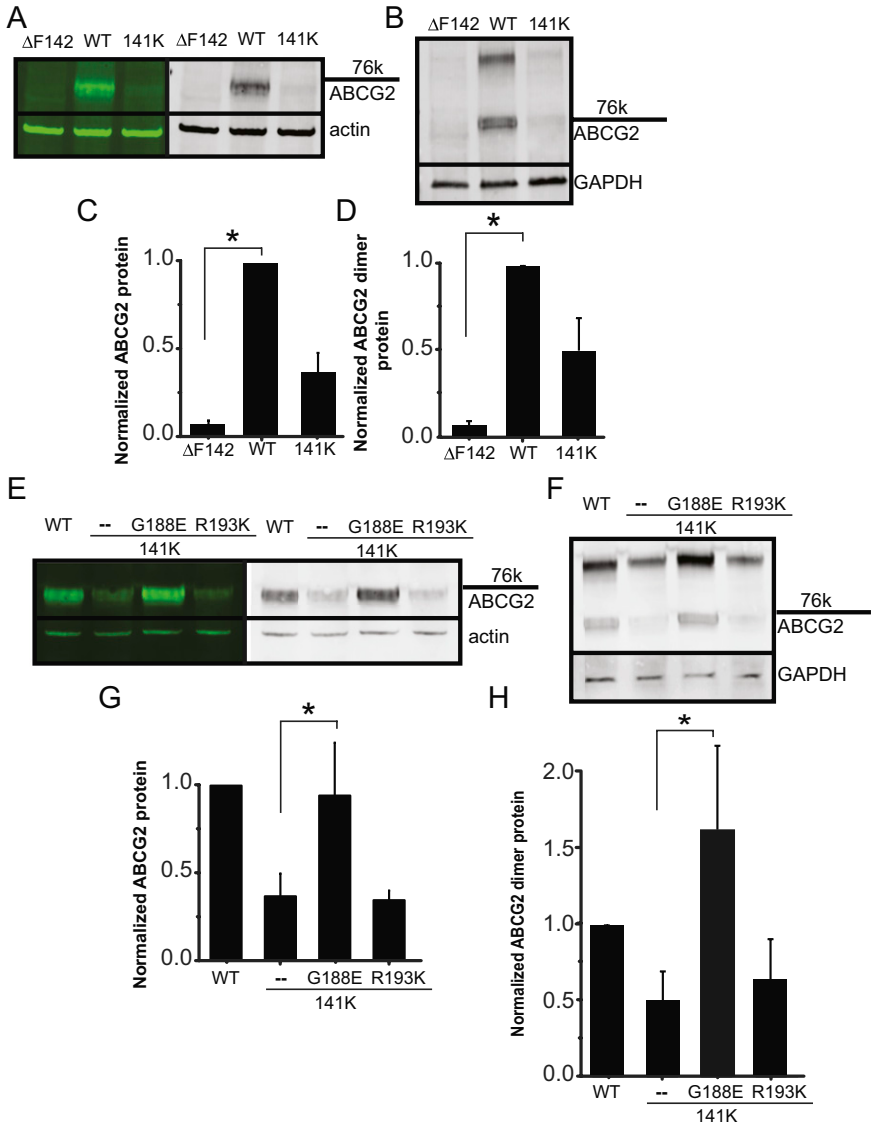

Fig. S4. (*A–D*) Western blot using a secondary fluorescent detection method allows for greater dynamic range and quantification of protein levels. Using the Bio-Rad Pharos FX fluorescent imaging system with Bio-Rad Quality One software, we confirmed that the deletion of F142 results in a severe and significant reduction in ABCG2 protein expression as a monomer or dimer compared with wild type. Likewise, quantitative Western technique confirms that the 188E mutation acts as a suppressor mutation for the Q141K mutant and significantly increases mutant protein expression (*E–H*). Experiments were done with HEK cells; $n = 3$ for each set of experiments. GAPDH and β-actin expression were used as a loading control on all Western blots. All means are ± SEM; $^*P < 0.05$.

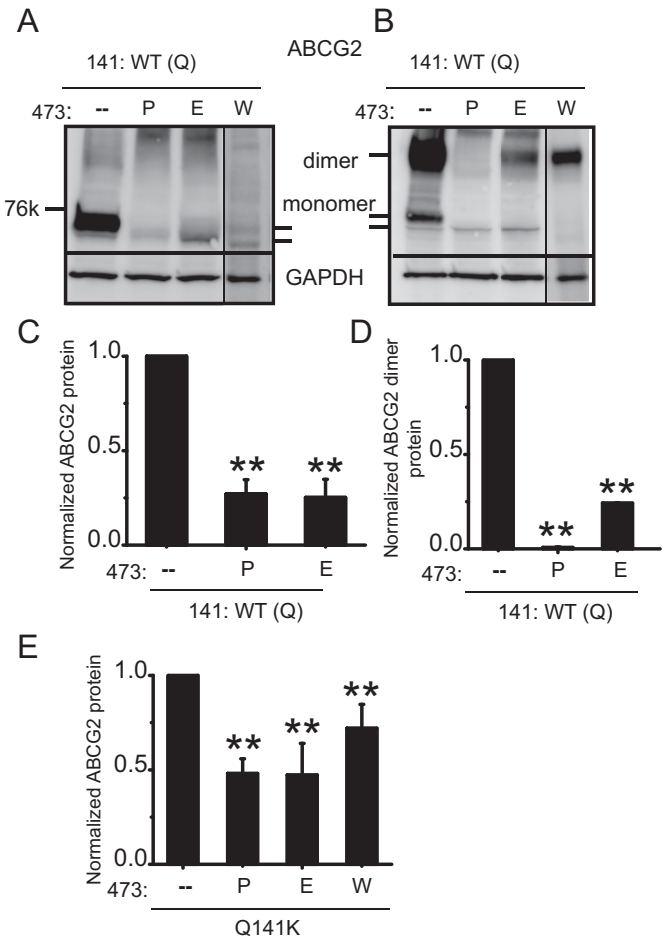

Fig. S5. Western blots of wild type (WT) ABCG2 expression in HEK293 cells with mutations at position K473 demonstrating the importance of the 473 side chains for total (*A*) and dimer (*B*) expression. Summary data of K473 mutations on total (*C*; $n = 3$) and dimer (*D*; $n = 2–4$) WT ABCG2 expression. (*E*) Summary data of K473 mutations on dimer Q141K expression (Western blot in Fig. 4*C*; $n = 4–6$). All means are ± SEM; $^{**}P < 0.01$.

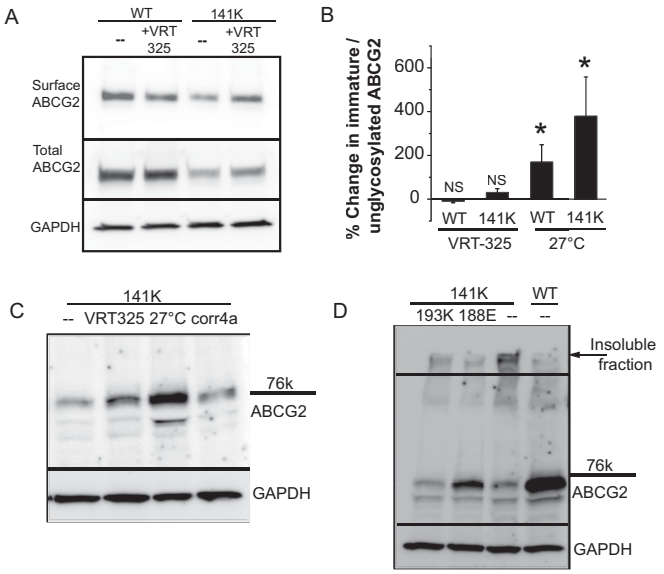

Fig. S6. (*A*) Western blot demonstrating that VRT-325 rescues surface-biotinylated Q141K ABCG2 expression ($n = 3$). (*B*) VRT-325 treatment does not increase the expression of immature, unglycosylated wild-type (WT) or Q141K ABCG2 ($n = 3$–4)—low-temperature rescue does ($n = 4$). (*C*) Comparison of correction of mutant Q141K protein expression in CHO cells using 24-h treatment of VRT-325 (10 μM), corr-4a (20 μM), and 27 °C incubation. (*D*) Representative Western blot illustrating the large fraction of insoluble/large-molecular-weight Q141K ABCG2 protein that is trapped at the top of the gel and appears at the top of the blot (black arrow); note that the amount in both suppressor mutation lanes is far less than for Q141K alone ($n = 3$). GAPDH expression was used as a loading control on all Western blots. All means are ± SEM; $^*P < 0.05$; NS, not significant.